Free Radical Biology and Medicine 177 (2021) 370–380

Contents lists available at ScienceDirect

Free Radical Biology and Medicine

journal homepage: www.elsevier.com/locate/freeradbiomed

Low cardiac content of long-chain acylcarnitines in TMLHE knockout mice prevents ischaemia-reperfusion-induced mitochondrial and cardiac damage

Edgars Liepinsh [a,*], Janis Kuka [a], Karlis Vilks [a], Baiba Svalbe [a], Gundega Stelfa [a], Reinis Vilskersts [a,b], Eduards Sevostjanovs [a], Niks Ricards Goldins [b], Valerija Groma [b], Solveiga Grinberga [a], Mario Plaas [c], Marina Makrecka-Kuka [a], Maija Dambrova [a,b]

[a] Latvian Institute of Organic Synthesis, Aizkraukles Str 21, Riga, LV1006, Latvia
[b] Riga Stradins University, Dzirciema Str 16, Riga, LV1007, Latvia
[c] Laboratory Animal Center, University of Tartu, Ravila 14b, Tartu, 50411, Estonia

ARTICLE INFO

Keywords:
Fatty acid metabolism
Myocardial infarction
PUFA
Acylcarnitine
Trimethyllysine
Gamma-butyrobetaine

ABSTRACT

Increased tissue content of long-chain acylcarnitines may induce mitochondrial and cardiac damage by stimulating ROS production. N^6-trimethyllysine dioxygenase (TMLD) is the first enzyme in the carnitine/acylcarnitine biosynthesis pathway. Inactivation of the *TMLHE* gene (TMLHE KO) in mice is expected to limit long-chain acylcarnitine synthesis and thus induce a cardio- and mitochondria-protective phenotype. *TMLHE* gene deletion in male mice lowered acylcarnitine concentrations in blood and cardiac tissues by up to 85% and decreased fatty acid oxidation by 30% but did not affect muscle and heart function in mice. Metabolome profile analysis revealed increased levels of polyunsaturated fatty acids (PUFAs) and a global shift in fatty acid content from saturated to unsaturated lipids. In the risk area of ischemic hearts in TMLHE KO mouse, the OXPHOS-dependent respiration rate and OXPHOS coupling efficiency were fully preserved. Additionally, the decreased long-chain acylcarnitine synthesis rate in TMLHE KO mice prevented ischaemia-reperfusion-induced ROS production in cardiac mitochondria. This was associated with a 39% smaller infarct size in the TMLHE KO mice. The arrest of the acylcarnitine biosynthesis pathway in TMLHE KO mice prevents ischaemia-reperfusion-induced damage in cardiac mitochondria and decreases infarct size. These results confirm that the decreased accumulation of ROS-increasing fatty acid metabolism intermediates prevents mitochondrial and cardiac damage during ischaemia-reperfusion.

1. Introduction

The accumulation of long-chain acylcarnitines induces mitochondrial dysfunction during ischaemia-reperfusion, heart failure and inherited disorders [1–3]. In the fatty acid metabolism pathway, the long-chain acylcarnitines are the main players in ROS production [4]. The mitochondrial enzyme carnitine palmitoyltransferase (CPT) 1 catalyses acylcarnitine synthesis from carnitine and long-chain acyl--coenzyme A (CoA) and is a rate-limiting step in long-chain fatty acid transport and oxidation [5]. CPT1 activity is independent of mitochondrial metabolic status but is regulated by the AMP-activated protein kinase (AMPK) and insulin signalling pathways through changes in malonyl-CoA concentration [6]. Despite the limited mitochondrial metabolism of acylcarnitines in CPT2-coupled β-oxidation during ischaemia, intracellular signals still facilitate CPT1 activity and acylcarnitine synthesis [7]. This leads to an increase in long-chain acylcarnitine content in the mitochondrial intermembrane space [7]. A high level of long-chain acylcarnitines in the mitochondria inhibits oxidative phosphorylation and induces ROS production [4,7,8]. In addition, long-chain acylcarnitines at physiological concentrations inhibit the cardioprotective PI3K-Akt pathway, related glucose uptake and pyruvate oxidation in mitochondria [9,10]. To prevent disturbances in cardiac metabolism, decreased long-chain acylcarnitine content is suggested as a potential treatment strategy for ischaemic heart disease [4,11].

Since carnitine is a substrate in acylcarnitine production, an effective strategy to inhibit the synthesis of long-chain acylcarnitines is a decrease in carnitine availability. Indeed, a reduced level of acylcarnitines was

* Corresponding author.
E-mail address: ledgars@farm.osi.lv (E. Liepinsh).

https://doi.org/10.1016/j.freeradbiomed.2021.10.035
Received 19 August 2021; Received in revised form 17 September 2021; Accepted 27 October 2021
Available online 30 October 2021

observed in response to inhibited carnitine synthesis and transport [12,13]. Pharmacological interventions that prevent acylcarnitine accumulation in various pathological states of mitochondrial dysfunction have been shown to reduce myocardial infarction, atherosclerosis and diabetes [12,14,15]. Similarly, CPT1 inhibition by oxfenicine treatment resulted in improved whole-body glucose tolerance and insulin sensitivity in a diet-induced insulin resistance model [16]. Decreases in long-chain acylcarnitine content using genetically modified carnitine and acylcarnitine biosynthesis enzymes have never been used to verify the beneficial effects of decreased acylcarnitine levels.

N^6-trimethyllysine (TML) dioxygenase (TMLD) hydroxylates TML to 3-hydroxy-TML [17]. TMLD is a nonheme ferrous-iron dioxygenase that requires 2-oxoglutarate, Fe^{2+} and molecular oxygen as cofactors [18]. TMLD was shown to localize in the mitochondrial matrix, and this enzyme is found in all tissues [19,20]. Since it is the first enzyme in the carnitine/acylcarnitine biosynthesis pathway, a decrease in TMLD activity would lower the levels of all its reaction products and downstream metabolic intermediates, including long-chain acylcarnitines. Therefore, we developed constitutive whole-body *TMLHE* gene mutant (TMLHE KO) mice to confirm the hypothesis that reduced long-chain acylcarnitine content prevents mitochondrial and cardiac damage in cases of myocardial infarction.

2. Materials and methods

2.1. Development of TMLHE KO mice model

The TMLHE KO mouse model was created in the Laboratory Animal Centre of Tartu University using the CRISPR/Cas9 gene-editing protocol to generate random mutations. Chemically modified CRISPR Revolution EZ sgRNA kit (TMLHE2.1 AGUUGUUGCACCAACAAAGC, Synthego Corporation, USA) and CRISPR Evolution Cas9 2NLS nuclease protein (Synthego Corporation) were used to target exon 2 of the *TMLHE* gene. Embryo electroporation (dpc 0.5 fertilized egg cells) was performed using an in-house validated protocol using a Nepagene Nepa21 electroporator and a CUY501P1-1.5 electrode. Following electroporation parameters were used: Poring pulse: voltage - 50 V, pulse length - 2.5 ms, interval - 50 ms, number of pulses - 4, decay rate - 10%, polarity (+); Transfer pulse: voltage - 5 V, pulse length - 50 ms, interval - 50 ms, number of pulses - 5, decay rate - 40%, polarity (±). The resulting founder lines were analysed by pyrosequencing to detect random mutations in exon 2 of the *TMLHE* gene. The most successful founder TMLHE knockout line had a deletion of 2 nucleotides, 103352 and 103353, located on the second coding exon in the TMLHE gene (NT_165789 REGION: 251286..469175). Nucleotides missing in TMLH KO animals resulted in a frameshift and multiple STOP codons after the first 13 amino acid coding triplets.

Male adult (8–12 weeks old) C57BL/6N mice (37 wild-type (WT) and 37 TMLHE KO) were housed under standard conditions (21–23 °C, reversed 12-hr light/dark cycle, relative humidity of 45–65%) with unlimited access to food (R70 diet from Lantmännen) and water. Generation of the TMLHE knockout mouse line was approved by the Estonian Project Authorisation Committee for Animal Experiments (No 103, 22nd of May 2017). Studies were only performed with male mice to eliminate the possible confounding effects of reproductive hormones. The experimental procedures were performed in accordance with the guidelines of the European Community and local laws and policies (Directive 2010/63/EU), and all of the procedures were approved by Food and Veterinary Service, Riga, Latvia. All experiments were performed in a blinded manner. Studies involving animals are reported in accordance with the ARRIVE guidelines [21].

2.2. TMLD activity assay

TMLD activity was assayed by measuring the formation of 3-hydroxy-TML from TML in mouse liver mitochondria *ex vivo*. Mitochondria from the liver were isolated as described previously [22]. The reaction mixture (final volume of 0.2 ml) contained the following: 20 mM potassium phosphate (pH 7.0), 20 mM potassium chloride, 3 mM 2-oxoglutarate, 0.25 mM ferrous ammonium sulfate, 10 mM sodium ascorbate, 0.16 mg of catalase, 500 μM TML and 0.9 mg of mitochondrial protein. The reaction was initiated by the addition of mitochondria, and the mixture was incubated at 37 °C for 2 h. The reaction was stopped by the addition of 0.2 ml of water and freezing in liquid nitrogen. Then, the mitochondria were lysed by 3 freeze-thaw cycles. After that, to perform deproteinization and extraction of HTML acetonitrile: methanol (1:3) was added and samples were centrifuged at 20000×*g* for 10 min. HTML and TML levels were measured by ultra-performance liquid chromatography-tandem mass spectrometry (UPLC-MS/MS) in positive ion electrospray mode [23].

2.3. Contents of GBB, carnitine and acylcarnitine

The concentrations of γ-butyrobetaine (GBB) and carnitine in plasma samples were measured by UPLC-MS/MS using positive ion electrospray mode [12]. The acylcarnitine profile in heart tissue and plasma samples was determined by UPLC-MS/MS as previously described [24].

2.4. Metabolomics and lipidomics

Metabolomic analysis was performed by Biocrates Life Sciences AG (Innsbruck, Austria), 630 metabolites were analysed in fed and overnight fasted mouse plasma samples using LC-MS/MS and an MxP® Quant 500 kit.

2.5. Fatty acid oxidation in isolated mice heart

The rate of radiolabelled palmitate oxidation was measured in isolated mouse hearts as previously described [25]. Briefly, mouse hearts were retrogradely perfused (perfusion pressure 70 mmHg) with the respective non-labelled oxygenated (95% O_2, 5% CO_2) Krebs-Henseleit (KH) buffer solution supplemented with 10 mM glucose, 0.3 mM sodium palmitate bound to 0.5% bovine serum albumin (BSA), 2 mM lactate, 0.2 mM pyruvate and 3 ng/ml insulin. After 20 min, the hearts were perfused with the respective oxygenated radiolabelled KH buffer solution for 10 min. The perfusate was collected to determine the fatty acid oxidation (FAO) rate by measuring the ^3H_2O released from [9,10-^{3}H]-palmitate (specific activity, 60 Ci/mmol) using the method described previously [25].

2.6. Transthoracic echocardiography in mice

The mice were anaesthetized using 5% isoflurane dissolved in oxygen. After the onset of anaesthesia, the concentration of isoflurane was decreased to 2.0%, the experimental animals were then placed in a decubitus position on a near-infrared heating pad to maintain body temperature. The fur from the chest was removed using commercially available depilation cream (Veet®). M-mode tracings of the left ventricle were recorded at the level of papillary muscles with an iE33 ultrasonograph equipped with a linear L15-7io transducer (Philips Healthcare, Andover, USA).

2.7. Myocardial infarction assay

Myocardial infarction was performed according to the Langendorff technique as described previously [26,27], with modifications required for mouse heart perfusion [28] as described below. The animals were anaesthetized with sodium pentobarbital (70 mg/kg), and heparin was administered intraperitoneally; after the loss of nociceptive reflexes, the hearts were immediately excised, sacrificing animals. Hearts were trimmed and mounted in the Langendorff system (ADInstruments) within 2 min of the excision. Hearts were retrogradely perfused with

oxygenated (95% O_2, 5% CO_2) KH buffer solution supplemented with 10 mM glucose (Fresenius Kabi), 0.2% BSA (FA-free) (Life Science Production LSG Ltd), and 3 ng/ml insulin (Novo Nordisk) at a constant perfusion pressure of 70 mmHg. After catheter tubing (0.7 mm) was inserted in the left ventricle apex wall to aid fluid drainage [28], a water-ethanol mixture (1:1)-filled balloon connected to a physiological pressure transducer (ADInstruments) was inserted into the left ventricle, and the baseline end-diastolic pressure was set at 5–10 mmHg. After an adaptation period of 20 min, the left anterior descending coronary artery (LAD) was subsequently occluded (Surgipro II 5-0 suture placed through the heart around the LAD and tightened) for 20 min followed by 120 min of reperfusion. Heart functional parameters: coronary flow, left ventricle developed pressure (LVDP), heart rate (HR) and cardiac workload were measured using the PowerLab system from ADInstruments. Infarct size was determined as described previously [27]. Briefly, at the end of reperfusion, the LAD was reoccluded, and the heart was perfused with 0.1% methylene blue dissolved in KH buffer solution to delineate risk and no-risk areas. Afterwards, the ventricles of the heart were transversely cut into 1.5 mm thick slices (four) and photographed. Computerized planimetric analysis of the stained left ventricle slice photographs was performed using Image-Pro Plus v6.3 software to determine the area at risk and the area of necrosis, and each area was expressed as a percentage of the slice area. The obtained values were then used to calculate the infarct size as a percentage of the risk area.

2.8. Mitochondrial functionality assessment

The infarction study was performed as described above. Animals were anaesthetized with sodium pentobarbital (70 mg/kg), and heparin was administered intraperitoneally; after the loss of nociceptive reflexes, the hearts were immediately excised, sacrificing animals. The hearts were perfused with oxygenated (95% O_2, 5% CO_2) KH buffer solution supplemented with 10 mM glucose, 0.2% bovine serum albumin, and 3 ng/ml insulin at a constant perfusion pressure of 70 mmHg. The isolated mouse hearts were adapted for 20 min, and the LAD was subsequently occluded for 20 min followed by shortened reperfusion for 60 min. After reperfusion, tissues were sectioned to obtain material from the risk area and non-risk area [27]. The permeabilized cardiac fibres were prepared from risk (ischaemic) areas and non-risk areas as described previously [29]. Mitochondrial respiration and H_2O_2 production measurements were performed at 37 °C using Oxygraph-2k (O2k; Oroboros Instruments, Innsbruck, Austria) with O2k-Fluo-Modules in MiR05 medium (110 mM sucrose, 60 mM K-lactobionate, 0.5 mM EGTA, 3 mM $MgCl_2$, 20 mM taurine, 10 mM KH_2PO_4, 20 mM HEPES, pH 7.1, 0.1% BSA (FA-free)). The medium was reoxygenated when the oxygen concentration decreased to 80 μM. H_2O_2 flux was measured simultaneously with respirometry in the O2k-Fluorometer using the H_2O_2-sensitive probe Ampliflu™ Red (AmR) as described [12]. The H_2O_2/O flux ratio [%] was calculated as the H_2O_2 flux/(0.5 O_2 flux).

Pyruvate and malate (5 mM and 2 mM, respectively) were used to determine NADH (N)-pathway, Complex I (CI)-linked LEAK respiration. Adenosine diphosphate (ADP) was added at a 5 mM concentration to determine oxidative phosphorylation-dependent respiration (OXPHOS state). Then, succinate (10 mM, Complex II (CII) substrate, S-pathway) was added to reconstitute convergent NS-pathway, CI- and CII-linked (CIII-linked) respiration. Then, an inhibitor of adenine nucleotide translocator (ANT), carboxyatractyloside (CATR), was added to determine $LEAK_{CATR}$ respiration.

In addition, FAO-dependent mitochondrial respiration in cardiac fibres was measured using palmitoylcarnitine (10 μM) and 0.5 mM malate as substrates. ADP was added to a concentration of 5 mM to assess respiration in the OXPHOS state. Pyruvate (5 mM, CI substrate, NADH (N)-pathway) was then added to reconstitute FN pathway-linked respiration. Succinate (10 mM, CII substrate, S-pathway) was added to reconstitute convergent FNS-linked respiration. Then, rotenone (Rot) (0.5 μM, inhibitor of CI) and antimycin A (2.5 μM, inhibitor of CIII) were added to determine the S-linked respiration and residual oxygen consumption (ROX), respectively.

The OXPHOS coupling efficiency was calculated as follows:

$$1 - \frac{Resp.rate\ LEAK\ state}{Resp.rate\ OXHOS\ state}$$

2.9. Preparation of cardiac muscle cells for assessment of mitochondrial ultrastructure

Hearts were obtained from four WT and four KO anaesthetized and sacrificed animals following transcardial perfusion-based fixation to rapidly and uniformly preserve the tissue. Perfusion was performed with approximately 50 ml of 4% paraformaldehyde fixative for 10 min. The perfusion pressure was continuously maintained at 130 mmHg. Immediately after perfusion fixation, the heart was isolated, cut into slices approximately 5 mm in thickness, and then into cubes with 1-mm sides. Then, the cubes were immersed in fixative containing 2.5% glutaraldehyde in 0.1 M cacodylate buffer for at least 24 h. Thereafter, the specimens were subjected to a standard preparation protocol where specimens were postfixed with 1% OsO_4, stained en bloc with uranyl acetate in maleate buffer at pH 5.2, dehydrated with ascending concentrations of ethanol, infiltrated, and embedded in Epon resin, which was subsequently polymerized at 62 °C for 24 h. Semithin sections of 1 μm thickness were cut and stained with 1% toluidine blue. Thereafter, ultrathin sections with a thickness of 60 nm were cut with an ultramicrotome (LKB Ultrotome V), mounted to 200-mesh copper grids, and double stained with 2% uranyl acetate in 70% methanol for 10 min, followed by lead citrate for 4 min. The specimens were imaged with a JEM 1011 JEOL (Japan) transmission electron microscope operating at 100 kV. Cardiac muscle cells were examined at ×8000 - 30000 magnification. Test fields were selected at a primary magnification of ×3000 by systematic uniform random sampling. Images were captured at ×8000 to analyse mitochondrial ultrastructure. For quantitative planimetric analysis, the imaged mitochondria were further analysed using Image-Pro Plus 6.3 software.

2.10. Statistical methods and exclusion criteria

Data are presented as the mean ± standard error of the mean (SEM). Based on data normality analysis, statistically significant differences in the mean values were evaluated using one-way ANOVA or the Kruskal-Wallis test. Based on data normality analysis, a *t*-test or the Mann Whitney test was used when only two groups were compared. If ANOVA or Kruskal-Wallis test yielded $P < 0.05$, Tukey's or Dunn's test was performed, respectively. Chi Square test was used for testing relationships between categorical variables. The differences were considered significant when $P < 0.05$. The data were analysed using GraphPad Prism statistical software (GraphPad Inc., San Diego, CA, USA). The exclusion criterion for experiments using the Langendorff-perfused isolated heart model was mounting time. Thus, if the heart could not be mounted within 4 min of excision, it was not included in the study. None of the hearts had to be excluded, as the mounting time was approximately 2 min.

3. Results

3.1. TMLHE KO mouse phenotype

The genotype for each mouse was confirmed using PCR (Fig. S1). To evaluate changes induced by loss-of-function of the TMLHE gene, TMLD enzyme activity was compared in liver samples from WT and TMLHE KO mice. In WT mice, liver TMLD enzyme activity was approximately 7 μU/mg prot, while in KO mice, liver TMLD was completely inactive (Fig. 1A). The absence of TMLD activity resulted in approximately by 90% lower concentrations of GBB and carnitine in plasma (Fig 1BC). As a result of limited carnitine availability, short-, medium- and long-chain

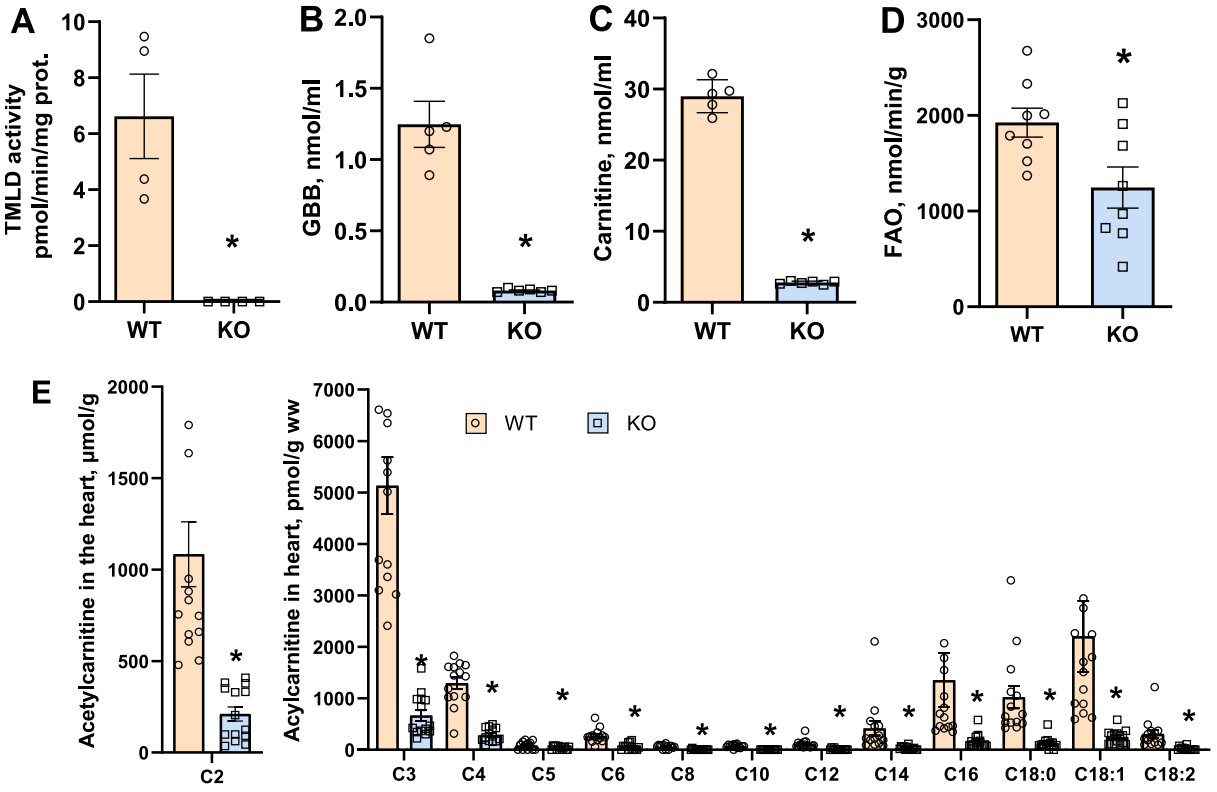

Fig. 1. Measurements of TMLD enzyme activity and GBB, carnitine, FAO and acylcarnitine concentrations in male WT and TMLHE KO mice. Liver TMLD enzyme activity was diminished in TMLHE KO mice compared to WT mice (A), and plasma concentrations of GBB (B) and carnitine (C) and cardiac contents of acylcarnitines (E) were significantly lower in KO mice. Overall cardiac fatty acid oxidation rate (FAO) was significantly lower in TMLHE KO mice (D). Each value is the mean ± SEM of 4–14 mice. *Significantly different from the WT group (Mann Whitney (A), *t*-test (B–E), $P < 0.05$). Abbreviations: TMLD, TML dioxygenase; GBB, γ-butyrobetaine; FAO fatty acid oxidation.

acylcarnitine contents in the heart were significantly decreased by 86%, 63% and 82%, respectively (Fig. 1E). The differences in the plasma acylcarnitine profile of KO and WT mice were the same (Fig. S2). The levels of plasma glucose, fatty acids and triglycerides in the plasma and liver were similar in WT and KO mice (Fig. S3). In addition, we compared the fatty acid oxidation rate in isolated intact mouse hearts of WT and KO mice. In KO animals, the [^{3}H]-palmitate oxidation rate in the heart was significantly decreased by 35% (Fig. 1D). In the animal behavior tests, we observed that both muscular coordination and motor function of adult and aged (20 month old) KO mice are completely preserved (see supplementary video file). Overall, these measurements confirm that TMLHE gene mutation resulted in significantly lower acylcarnitine levels and a reduced risk of acylcarnitine accumulation in the mitochondria without any detrimental effects on muscle functions.

3.1.1. *The functionality of the intact heart in vivo and ex vivo*

To evaluate whether lower acylcarnitine levels and FAO rate influence cardiac functionality, anatomical and functional parameters of the left ventricle were assessed using echocardiography. As shown in Fig. S4, the ejection fraction (EF) and fractional shortening (FS) of the left ventricle were similar in both groups. The EFs in the control and TMLHE KO groups were 70 ± 1% and 68 ± 2%, respectively. The FS values in the control and TMLHE KO groups were 34 ± 1% and 33 ± 2%, respectively. Additionally, there were no differences in the thicknesses of the interventricular septum at end-systole (IVSs), interventricular septum at end-diastole (IVSd), left ventricular posterior wall at end-systole (LVPWs), and left ventricular posterior wall at end-diastole (LVPWd). Similarly, in Langendorff-perfused isolated hearts, the functional parameters coronary flow, left ventricular developed pressure, HR and contractility (dp/dt max) were not significantly different between WT and TMLHE KO mice (Fig. S4). Overall, lower acylcarnitine levels and reduced FAO rate did not influence intact heart functionality in TMLHE KO mice.

3.2. *Metabolomic analysis*

In the metabolomics (lipidomics) analysis of plasma samples from fed and overnight fasted mice, the most significantly changed metabolites in TMLHE KO mice were short-, medium-, and long-chain acylcarnitines (Fig. 2A). Additionally, according to whole lipidome data, lipids mostly consisting of saturated or monounsaturated FA were markedly decreased by up to 40% in TMLHE KO compared to WT mouse plasma, while lipids consisting of more than 6 double bonds were increased by up to 80% (Fig. 2B). Nevertheless, the total concentrations of lysophosphatidylcholine, phosphatidyl-cholines, sphingomyelins, ceramides, dihexosyl-ceramides, and cholesteryl esters were similar in WT and TMLHE KO mice (Fig. 2A). Thus, despite the same diet, in TMLHE KO mice, the lipid profile was markedly shifted to a significantly higher abundance of unsaturated FA (Fig. 2B). In the metabolome analysis of individual FA, we found increased concentrations of PUFAs in the plasma of TMLHE KO mice (Fig. 2B). In the fed TMLHE KO mice, plasma concentrations of eicosapentaenoic acid (EPA) and docosahexaenoic acid (DHA) were increased by approximately 35% (Fig. 2CD). In the fasted state, DHA and EPA concentrations in plasma were 1.5- and 2.2-fold higher than those in the corresponding WT control group, respectively (Fig. 2CD). In contrast, the concentrations of palmitate and other non-esterified saturated FA in TMLHE KO mouse plasma were not higher than those in WT mouse plasma (Fig. 2E and Fig. S3). The measurements of non-lipid metabolites showed significant approximately 25% lower lactate and succinate concentrations in TMLHE KO mouse plasma (Fig. 2FG), indicating that mitochondrial metabolism of lactate/pyruvate and the Krebs cycle were increased in response to the lower

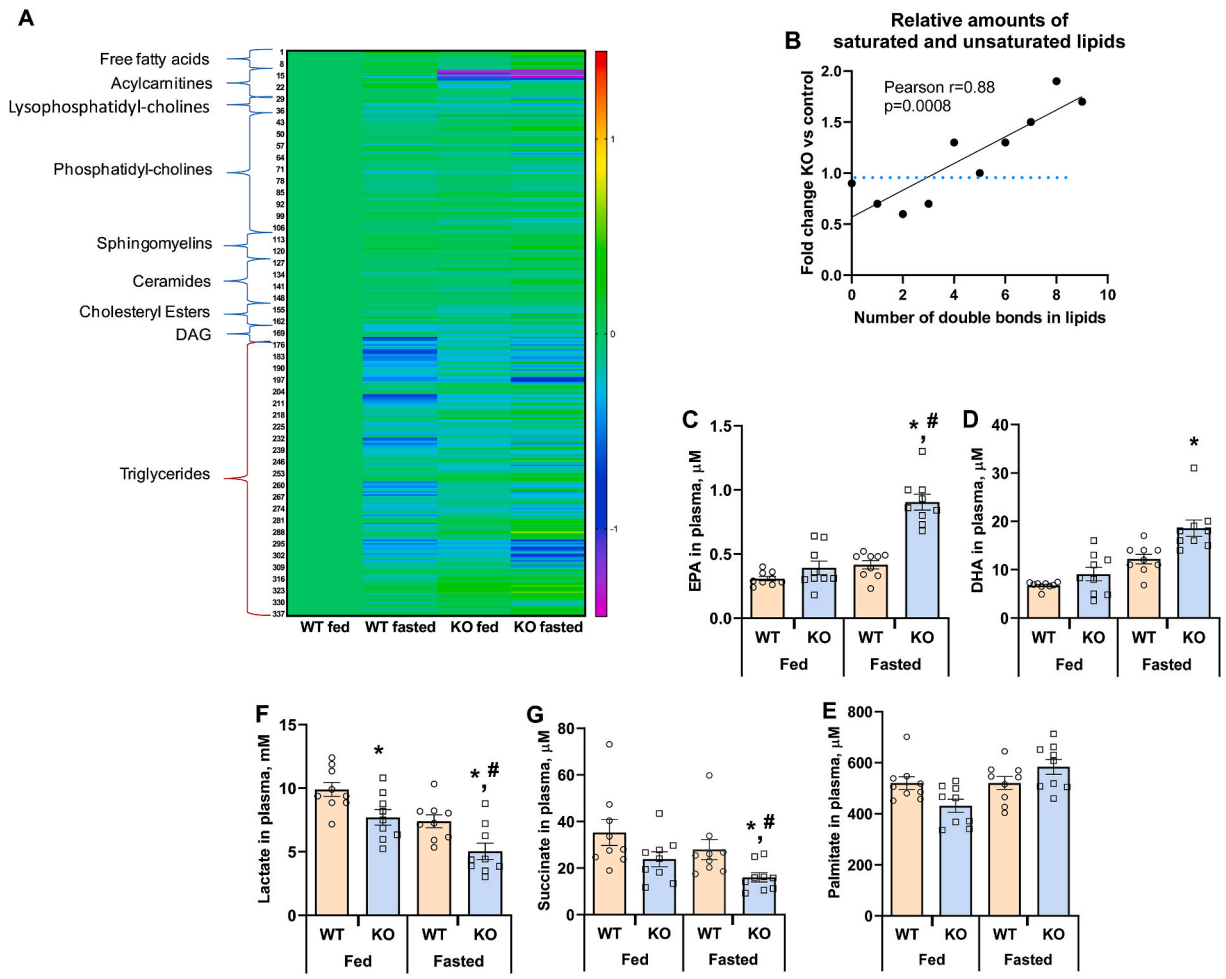

Fig. 2. Metabolomics analysis of male WT and TMLHE KO mice plasma. In total, 630 metabolites were analysed in WT and TMLHE KO mouse plasma samples using LC-MS/MS and the MxP® Quant 500 kit (Biocrates). The lipid metabolite profile presented as a heatmap (A) showed differences in acylcarnitine and PUFA concentrations and a global shift in FA content from saturated to unsaturated lipids (B). EPA (C) and DHA (D) concentrations in plasma were significantly higher in TMLHE KO mice in the fasted state than in the other groups, instead palmitate concentrations were significantly lower in TMLHE KO mice in the fed state (E). Lactate (F) and succinate (G) concentrations were lower in TMLHE KO mice in both states. Data are expressed as heatmap (values of metabolite concentrations were normalized to WT fed group) and as the mean ± SEM (n = 9 in each group). *Significantly different from the WT group in the fed state. #Significantly different from the WT group in the fasted state (Kruskall-Wallis test followed by Dunn's multiple comparisons test $P < 0.05$). Abbreviations: DAG, Diacylglycerols; EPA, eicosapentaenoic acid; DHA, docosahexaenoic acid.

long-chain acylcarnitine levels in TMLHE KO mice.

3.3. Myocardial infarction

In the myocardial ischaemia-reperfusion experiment, the area at risk in both WT and TMLHE KO mouse hearts was on average 56–60% of the left ventricle (Fig. 3A). The infarct size in WT mouse hearts was 49 ± 4.7%; in comparison, in TMLHE KO mice, the infarct size was 30 ± 3.6%, significantly smaller than that in WT mice (Fig. 3B). Thus, the hypothesis that a lower cardiac content of long-chain acylcarnitine levels is cardioprotective is confirmed for the first time in a genetic mouse model.

The heart functional parameters of isolated Langendorff-perfused hearts from TMLHE KO mice were similar to those hearts from WT mice (Fig. 3CD). Cardiac flow in the intact isolated heart was approximately 2 ml/min in both WT and TMLHE KO mice. Additionally, the LVDP, and the HR was similar in both groups (Fig. 3CD). Accordingly, cardiac work was similar in hearts isolated from TMLHE KO mice and WT mice. Coronary flow during LAD occlusion was decreased by 45% in the WT control mouse group and by 51% in the TMLHE KO mouse group. During reperfusion, coronary flow recovered up to 90% from baseline in the WT group and up to 115% in the TMLHE KO group, although this difference was not statistically significant. No significant differences were observed in LVDP, HR, or cardiac workload between the WT and TMLHE KO mouse groups during occlusion and reperfusion (Fig. 3CD).

3.4. Mitochondrial function

If compared with WT mice, in the cardiac fibres isolated from the non-risk area of TMLHE KO mouse hearts, the carnitine-independent CPT2-coupled β-oxidation of long-chain acylcarnitines as well as the pyruvate (N) or pyruvate and succinate (NS) pathway-linked respiration rate in the OXPHOS state was higher by 24–46% (Fig. 4AB); however, there was no difference in FAO-dependent and NS pathway-dependent OXPHOS coupling efficiency between TMLHE KO and WT animals (Fig. 4CD). In addition, under normoxic conditions, a similar rate of mitochondrial ROS production (H_2O_2/O ratio) was observed in both groups in all of the studied states and pathways (Fig. 4EF). These results indicate that limited carnitine availability in TMLHE KO animals does not inhibit but rather stimulates mitochondrial bioenergetics related to pyruvate and fatty acid metabolism.

Ischaemia-reperfusion induced significant disturbances in

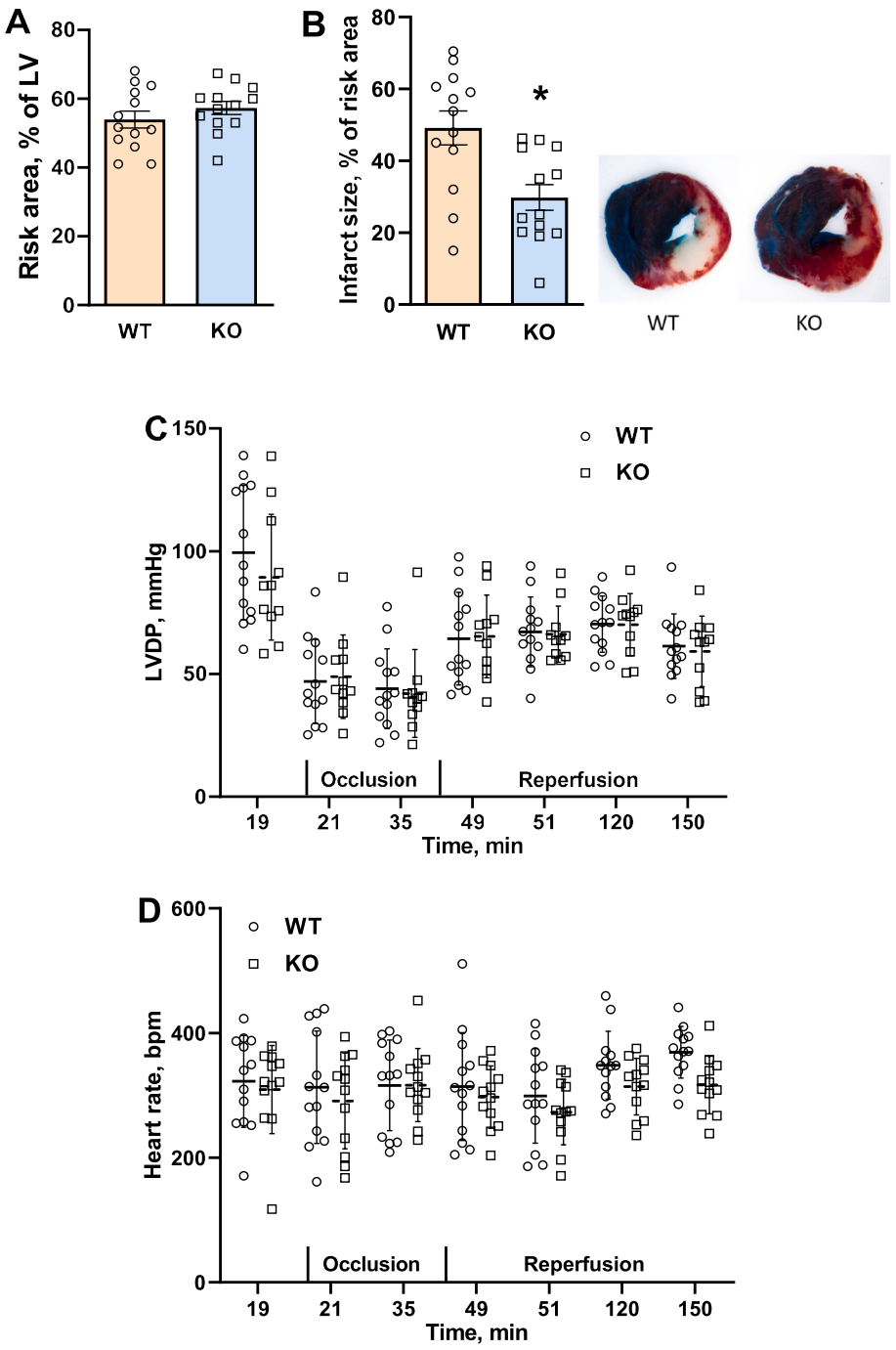

Fig. 3. Area at risk (A), infarct size (B), representative images of TTC-stained heart slices and the heart functional parameters LVDP (C) and heart rate (D) of male WT and TMLHE KO mice. Infarct size was determined in a Langendorff-perfused isolated heart ischaemia-reperfusion model. Data are expressed as the mean ± SEM (n = 11–13 in each group). Cardiac parameters were not recorded for 2 hearts in the KO group due to sensor failure *$p < 0.05$ vs. the corresponding WT control mice (*t*-test). Abbreviations: LV, left ventricle; LVDP, left ventricle developed pressure; TTC, triphenyl tetrazolium chloride.

mitochondrial functionality in WT mouse hearts. In cardiac fibers isolated from the risk area of WT mouse left ventricles, FAO-dependent and FN pathway respiration were decreased by approximately 75% (Fig. 4AB), while N- and NS-linked OXPHOS-dependent respiration rates were decreased by 73% and 52% (Fig. 4B), respectively. Moreover, in fibers from the risk area of WT animals, a significant 58% reduction in NS pathway-dependent OXPHOS coupling efficiency was observed (Fig. 4D), while in FAO-dependent OXPHOS, coupling efficiency tended to be decreased by 33% ($p = 0.12$). (Fig. 4C). As indicated by the H_2O_2/O ratio in WT animal cardiac fibers after ischaemia-reperfusion, the production of mitochondrial ROS in the OXPHOS state was increased by 3–13 times compared to fibers isolated from a non-risk area of the heart (Fig. 4EF).

In the risk area of KO mouse hearts, N- and NS-linked OXPHOS-dependent respiration rates, as well as OXPHOS coupling efficiency, were preserved under ischaemia-reperfusion damage (Fig. 4BD). Moreover, the H_2O_2/O ratio was significantly lower (on average, 2.3 times) in the FAO-, N- and NS-linked OXPHOS state in TMLHE KO risk areas compared to those in WT mice (Fig. 4EF). Taken together, these results indicate that in TMLHE KO mice, cardiac mitochondrial functionality is protected from ischaemia-reperfusion-induced damage. Overall, lower carnitine bioavailability combined with stimulated acylcarnitine utilization in mitochondria results in low levels of acylcarnitines and a lower risk of long-chain acylcarnitine-induced mitochondrial damage.

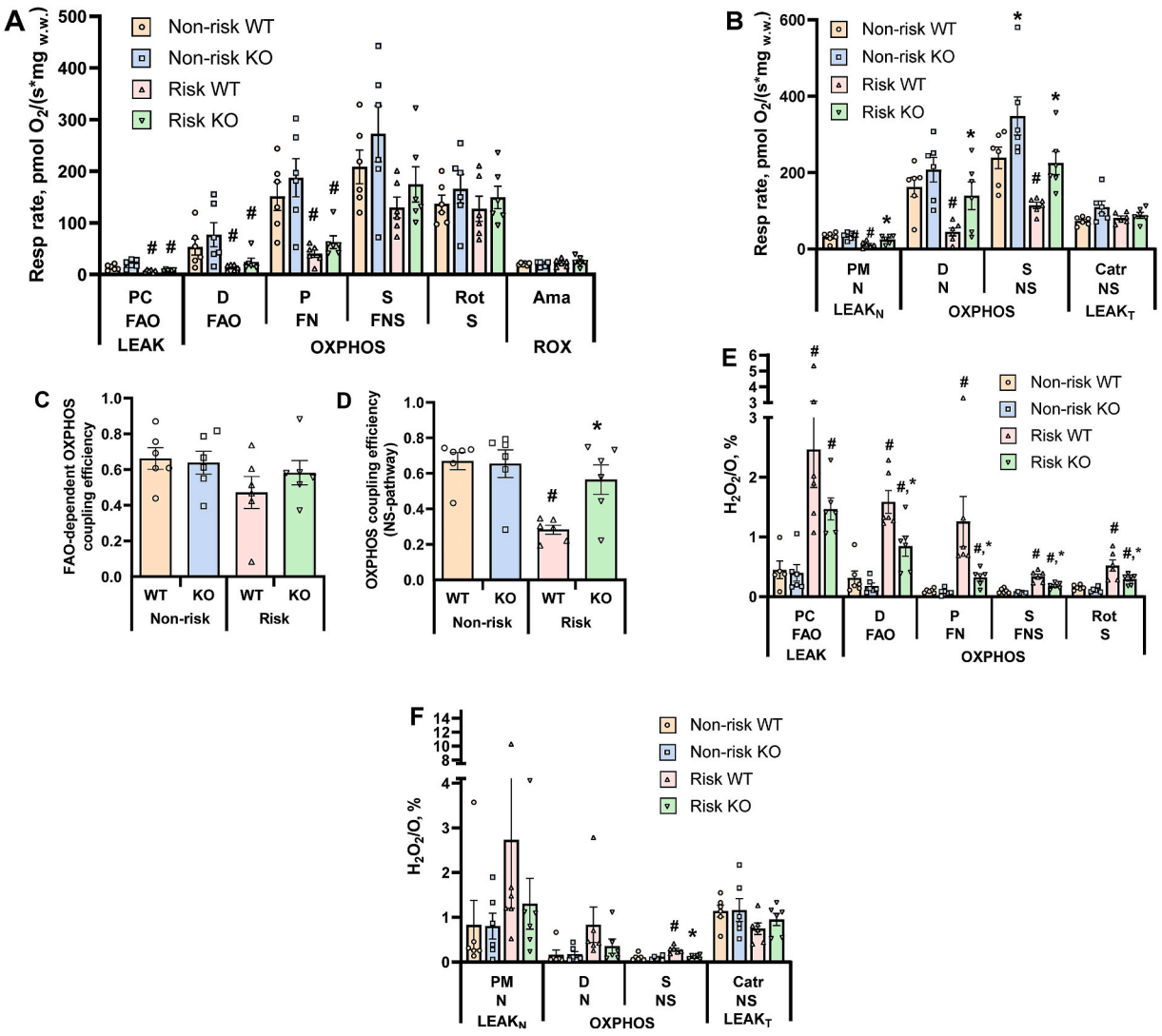

Fig. 4. Mitochondrial respiration rate (AB), OXPHOS coupling efficiency (CD), and mitochondrial ROS production (EF) in permeabilized cardiac fibers from normoxic non-risk and reperfused areas in at-risk regions of the male mice heart. Each value represents the mean ± SEM of 6 mice. *Significantly different from the respective WT control (NR or R) group (*t*-test, $P < 0.05$). #Significantly different from the respective normoxic (NR) group (*t*-test, $P < 0.05$). Abbreviations: PC, palmitoylcarnitine; FAO, fatty acid oxidation; OXPHOS, oxidative phosphorylation-dependent state; LEAK/$LEAK_N$, substrate metabolism-dependent state without adenylates; $LEAK_T$, LEAK in presence of ATP; D, ADP; PM, pyruvate and malate; FAO dependent pathway; N, NADH pathway; S, succinate pathway; Ama, Antimycin A; ROX, residual oxygen consumption; Catr, carboxyatractyloside; Rot, rotenone.

3.5. *Ultrastructure of cardiomyocyte mitochondria*

Since TMLD is a mitochondrial enzyme, the ultrastructural organization of the organelle was examined by transmission electron microscopy in both WT and TMLHE KO animals. No apparent ultrastructural changes in cardiac muscle cells were observed in TMLHE KO animals compared with WT mice. The numerous mitochondria were arranged in rows and interspersed by tightly packed contractile filaments that appeared to be thick myosin and thin actin filaments. In addition, cisternae of the smooth endoplasmic reticulum were near the outer mitochondrial membrane. The outer and inner mitochondrial membranes were intact, the intermembrane space was narrow, numerous lamellar cristae were densely packed, and the density of the matrix was moderate (Fig. 5A). Differently shaped and sized mitochondrial profiles were demonstrated in thin sections. Furthermore, according to quantification analyses, significantly more mitochondrial profiles per microscopic field were observed in cardiac muscle cells of TMLHE KO mice than in those of WT mice (Fig. 5B). Simultaneously, the mitochondrial area calculated for cardiac muscle cells was similar in WT and TMLHE KO mice (Fig. 5C). Finally, a significantly increased percentage of small mitochondria and a decreased percentage of large mitochondria were observed in the cardiac muscle cells of TMLHE KO mice compared to those of WT mice (Fig. 5D). Citrate synthase activity and the amount of mitochondrial DNA (Fig. 5EF), as well as the expression level of mitochondrial biogenesis and fission- and fusion-related genes, were similar in TMLHE KO and WT mouse hearts (Fig. S5). Taken together, these data demonstrate that deletion of mitochondrial TMLHE slightly increases the number of small mitochondria but does not substantially change mitochondrial biogenesis, fission-fusion, morphology, or organization in the heart.

4. Discussion

The inactivity of the TMLD enzyme in TMLHE KO mice resulted in an substantially lower long-chain acylcarnitine content in plasma and in the heart. Limited acylcarnitine biosynthesis induced a partial decrease in the cardiac FAO rate by 35% and a subsequent increase in the plasma concentrations of PUFAs but not saturated fatty acids. Other measures of

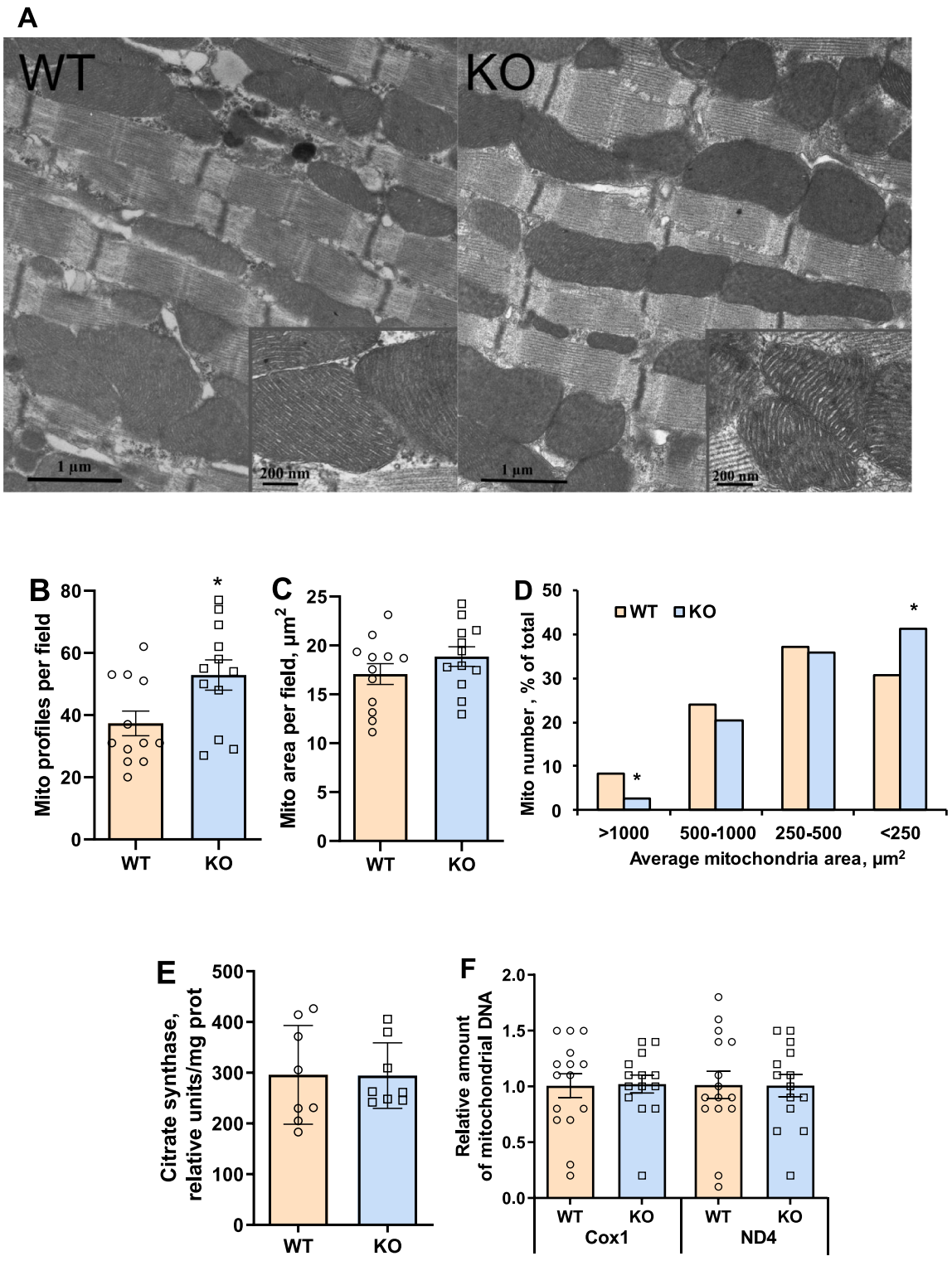

Fig. 5. Qualitative and quantitative assessment of mitochondrial ultrastructure. Representative transmission electron microscopy images of mitochondrial morphology in cardiac muscle cells of male WT and TMLHE KO mice (A). Electron micrographs of the cardiac muscle cells of both WT (left panel) and TMLHE KO (right panel) mice depict well-preserved mitochondrial features such as intact membranes and regularly organized cristae. Scale bars: 1 µm (200 nm, inserts). Mitochondrial morphology was assessed in cardiac muscle cells of WT and TMLHE KO mice and expressed as the average number of mitochondrial profiles per microscopic field (B). Mitochondrial area assessed per microscopic field in cardiac muscle cells of WT and TMLHE KO mice (C). Frequency of distribution according to size demonstrated in cardiac muscle cells of WT and TMLHE KO mice when an average value for the mitochondrial area was considered (D). If the square of a single mitochondrial profile exceeded 1000 µm^2, it was considered large, whereas if the square of a single profile was less than 250 µm^2, it was considered small. The amount of mitochondria was compared by measuring mitochondrial citrate synthase activity (E) and the amount of mitochondrial DNA (F) in the hearts of WT and KO mice. Mito − mitochondrion. Bars represent mean ± SEM. * Significantly different from the WT group (*t*-test (A), Chi-squared test (D), $P < 0.05$). Abbreviations: Cox1, Cytochrome *c* oxidase I; ND4, NADH dehydrogenase 4.

metabolic phenotype, mitochondrial number and morphology, and cardiac mechanic functionality were similar in TMLHE KO and WT mice. In the state of decreased acylcarnitine content, TMLHE KO mouse cardiac mitochondria have significantly better preserved functionality and a lower ROS production rate during ischaemia-reperfusion than WT mouse cardiac mitochondria. This coincided with a smaller infarct size in the TMLHE KO mice.

It has been demonstrated that long-chain acylcarnitines accumulate in the heart and substantially contribute to cardiac damage during ischaemia and reperfusion [7,13,30]. Thus far, the lowering of long-chain acylcarnitine levels has been achieved by pharmacological agents [12,26] that might have some off-target actions. In this study, a lower acylcarnitine content was achieved through genetic manipulation, and the absence of TMLD-driven acylcarnitine biosynthesis was associated with a 39% smaller infarct size in TMLHE KO mice than in WT mice. This is in line with previous studies showing the beneficial effect of reduced long-chain acylcarnitine content by pharmacological agents [12,26]. In the metabolomic analysis, a several-fold reduction in acylcarnitine content was the most prominent difference among more than 600 metabolites measured in TMLHE KO and WT mice. Thus, the effect on acylcarnitine content could be considered the main mechanism responsible for the cardioprotective effect in TMLHE KO mice. Additionally, the novel finding of this study is increased levels of unsaturated fatty acids, in particular, PUFAs, in TMLHE KO animals. Thus the decreased long-chain acylcarnitine production rate increases PUFA levels in TMLHE KO mice. It is widely accepted that the reduced risk of cardiovascular disease and type 2 diabetes, as well as other beneficial effects on health are observed when dietary saturated FA are replaced with PUFA [31]. The shift from saturated to unsaturated fatty acid content as well as a marked increase in DHA and EPA levels may be partially responsible for the cardioprotective phenotype in TMLHE KO mice.

During ischaemia, long-chain acylcarnitines are excessively generated, accumulate in mitochondria, and induce marked impairment in mitochondrial functionality [8,32]. In this study, in WT animals, we also found substantial OXPHOS inhibition in cardiac mitochondria from the area at risk. These unfavourable effects on mitochondria are typical for increased levels of long-chain acylcarnitines [7]. In contrast, in the risk area of TMLHE KO mouse hearts, the OXPHOS-dependent respiration rate and OXPHOS coupling efficiency were fully preserved against ischaemia-reperfusion damage. Thus, the reduced acylcarnitine biosynthesis rate in TMLHE KO mouse heart mitochondria prevents the accumulation of long-chain acylcarnitines and corresponding damage. This also confirms that long-chain acylcarnitine accumulation contributes to substantial mitochondrial damage during ischaemia-reperfusion. The effect on FAO-dependent respiration in the ischaemic area of TMLHE KO mouse heart mitochondria was somewhat less pronounced. It could be explained by the observation that oxygen consumption in the risk area of WT animal hearts is not fully coupled with oxidative phosphorylation and a part of oxygen is wasted for the formation of ROS. In KO animals ROS production is significantly reduced and coupling efficiency is significantly improved. Also, the decrease in CPT2-linked β-oxidation is partially caused by ischaemia-induced free CoA deficiency in mitochondria, which could be only partially prevented in the case of lower levels of acylcarnitines. Also, the decrease in CPT2-linked β-oxidation is partially caused by ischaemia-induced free CoA deficiency in mitochondria, which could be only partially prevented in the case of lower levels of acylcarnitines. Importantly, ROS production was similarly decreased in FAO-, pyruvate- and pyruvate & succinate metabolism-linked pathways, supporting the difference in the OXPHOS states of TMLHE KO and WT mice. This finding confirms the essential role of long-chain acylcarnitines in ROS induction during reperfusion. Taken together, these results suggest that long-chain acylcarnitines significantly contribute to mitochondrial functional disturbances, and a decrease in long-chain acylcarnitines prevents ischaemia-reperfusion-induced mitochondrial damage.

Carnitine is considered a pivotal molecule for the function of energy metabolism pathways [33]. In humans, primary carnitine deficiency is a rare autosomal recessive disorder most frequently caused by defective carnitine transport [34,35]. Impaired carnitine transport depletes long-chain fatty acid oxidation in mitochondria and can result in skeletal muscle myopathy and cardiomyopathy [35,36]. However, TMLD deficiency in humans is not causing any severe phenotype despite lower levels of GBB and carnitine [35,37]. In this study, limited carnitine availability in TMLHE KO mice reduced the fatty acid oxidation rate in the heart only by 35%; however, mitochondrial respiration via both pyruvate and palmitoylcarnitine was increased. This suggests that mitochondrial metabolism was enhanced through both main metabolic pathways. In the metabolomic analysis, we found lower levels of acetylcarnitine, lactate, and succinate, suggesting the complete mitochondrial metabolism [38,39] of energy substrates, while mitochondrial morphology, biogenesis, and fission-fusion were similar in WT and TMLHE KO mice. Importantly, despite the lower fatty acid oxidation rate, the cardiac functionality of TMLHE KO mice was unchanged, as evidenced by measurements in isolated heart experiments and echocardiography examinations *in vivo*. In addition, we observed completely preserved muscular coordination and motor function in the rotarod test of adult and aged (20-month-old) TMLHE KO mice (Supplementary video). Overall, a lower level of long-chain acylcarnitines before ischaemia in TMLHE KO optimizes pyruvate metabolism, β-oxidation, and Krebs cycle functioning, ensuring the complete metabolism of energy substrates and proper heart and muscle function.

TML and GBB are substrate and product of the TMLD enzyme, respectively. They are known mostly as bio-precursors of carnitine, while GBB availability is considered a limiting factor for carnitine biosynthesis [40]. To date, there are very few studies related to the physiological and pharmacological properties of GBB and TML. The metabolites of carnitine and GBB were first investigated for acetylcholine-like activity decades ago [41], but later, it was shown that the methyl ester of GBB but not GBB itself exerts its biological activity by binding to muscarinic acetylcholine receptors [42]. Recently, it was found that serum levels of TML, GBB, and long-chain palmitoylcarnitine predict the long-term risk of type 2 diabetes independently of traditional risk factors, possibly reflecting dysfunctional fatty acid metabolism in subjects susceptible to type 2 diabetes development [43]. In a study by Schooneman, GBB supplementation did not facilitate FAO and did not prevent impaired glucose homeostasis in HFD-fed mice [44]. In this study, up to a 10-fold decrease in GBB plasma concentration was observed in TMLHE KO mice, which led to lower levels of carnitine and acylcarnitines. However, except for the role of precursors of carnitine and following acylcarnitine synthesis, we cannot currently link TML and GBB to any other biochemical changes in TMLHE KO mice.

In conclusion, genetic inactivation of the TMLD enzyme in TMLHE KO mice resulted in significantly lower acylcarnitine content and a partial decrease in the cardiac FAO rate. In the plasma metabolome of TMLHE KO mice, mainly GBB, carnitine, and acylcarnitine levels were decreased, while PUFA concentrations were significantly increased. In the state of decreased long-chain acylcarnitine content, TMLHE KO mouse cardiac mitochondria have significantly preserved functionality and a lower ROS production rate after ischaemia-reperfusion than WT mice. Accordingly, loss of TMLD activity is associated with a significantly smaller infarct size in TMLHE KO mice and points to TMLD as a novel target for cardioprotective therapies.

Author contributions

Participated in research design: EL, MMK, MD. Development of KO mice model and breeding: MP, GS, BS. Conducted experiments: MMK, JK, RV, KV, VG, NRG. Analytical chemistry: ES, SG. Wrote or contributed to the writing of the manuscript: EL, MMK, MD, JK, RV, VG, NRG.

Sources of funding

This research was supported by the Latvian Council of Science, project TRILYSOX, grant No. LZP-2018/1-0082 and authors were supported by the European Union's Horizon 2020 research and innovation programme under grant agreement No 857394.

Declaration of competing interest

There is no conflict of interest.

Acknowledgements

We are thankful for the metabolomic analysis of plasma samples by Biocrates Life Sciences AG, Innsbruck, in particular by Wulf Fischer-Knuppertz.

Appendix A. Supplementary data

Supplementary data to this article can be found online at https://doi.org/10.1016/j.freeradbiomed.2021.10.035.

References

[1] C.S. McCoin, T.A. Knotts, S.H. Adams, Acylcarnitines–old actors auditioning for new roles in metabolic physiology, Nat. Rev. Endocrinol. 11 (10) (2015) 617–625.
[2] T. Ahmad, J.P. Kelly, R.W. McGarrah, A.S. Hellkamp, M. Fiuzat, J.M. Testani, T. S. Wang, A. Verma, M.D. Samsky, M.P. Donahue, O.R. Ilkayeva, D.E. Bowles, C. B. Patel, C.A. Milano, J.G. Rogers, G.M. Felker, C.M. O'Connor, S.H. Shah, W. E. Kraus, Prognostic implications of long-chain acylcarnitines in heart failure and reversibility with mechanical circulatory support, J. Am. Coll. Cardiol. 67 (3) (2016) 291–299.
[3] R.J.A. Wanders, G. Visser, S. Ferdinandusse, F.M. Vaz, R.H. Houtkooper, Mitochondrial fatty acid oxidation disorders: laboratory diagnosis, pathogenesis, and the complicated route to treatment, J Lipid Atheroscler 9 (3) (2020) 313–333.
[4] M. Dambrova, C.J. Zuurbier, V. Borutaite, E. Liepinsh, M. Makrecka-Kuka, Energy substrate metabolism and mitochondrial oxidative stress in cardiac ischemia/reperfusion injury, Free Radic. Biol. Med. 165 (2021) 24–37.
[5] L.P. Shriver, M. Manchester, Inhibition of fatty acid metabolism ameliorates disease activity in an animal model of multiple sclerosis, Sci. Rep. 1 (2011) 79.
[6] I.R. Schlaepfer, M. Joshi, CPT1A-mediated fat oxidation, mechanisms, and therapeutic potential, Endocrinology 161 (2) (2020).
[7] E. Liepinsh, M. Makrecka-Kuka, K. Volska, J. Kuka, E. Makarova, U. Antone, E. Sevostjanovs, R. Vilskersts, A. Strods, K. Tars, M. Dambrova, Long-chain acylcarnitines determine ischemia-reperfusion induced damage in heart mitochondria, Biochem. J. 473 (9) (2016) 1191–1202, https://doi.org/10.1042/BCJ20160164.
[8] H. Tominaga, H. Katoh, K. Odagiri, Y. Takeuchi, H. Kawashima, M. Saotome, T. Urushida, H. Satoh, H. Hayashi, Different effects of palmitoyl-L-carnitine and palmitoyl-CoA on mitochondrial function in rat ventricular myocytes, Am. J. Physiol. Heart Circ. Physiol. 295 (1) (2008) H105–H112.
[9] C. Aguer, C.S. McCoin, T.A. Knotts, A.B. Thrush, K. Ono-Moore, R. McPherson, R. Dent, D.H. Hwang, S.H. Adams, M.E. Harper, Acylcarnitines: potential implications for skeletal muscle insulin resistance, Faseb. J. : Off. Publ. Feder. Am. Soc. Exp. Biol. 29 (1) (2015) 336–345.
[10] M. Makrecka, J. Kuka, K. Volska, U. Antone, E. Sevostjanovs, H. Cirule, S. Grinberga, O. Pugovics, M. Dambrova, E. Liepinsh, Long-chain acylcarnitine content determines the pattern of energy metabolism in cardiac mitochondria, Mol. Cell. Biochem. 395 (1–2) (2014) 1–10.
[11] C.J. Zuurbier, L. Bertrand, C.R. Beauloye, I. Andreadou, M. Ruiz-Meana, N. R. Jespersen, D. Kula-Alwar, H.A. Prag, H. Eric Botker, M. Dambrova, C. Montessuit, T. Kaambre, E. Liepinsh, P.S. Brookes, T. Krieg, Cardiac metabolism as a driver and therapeutic target of myocardial infarction, J. Cell Mol. Med. 24 (11) (2020) 5937–5954.
[12] E. Liepinsh, M. Makrecka-Kuka, J. Kuka, R. Vilskersts, E. Makarova, H. Cirule, E. Loza, D. Lola, S. Grinberga, O. Pugovics, I. Kalvins, M. Dambrova, Inhibition of L-carnitine biosynthesis and transport by methyl-gamma-butyrobetaine decreases fatty acid oxidation and protects against myocardial infarction, Br. J. Pharmacol. 172 (5) (2015) 1319–1332.
[13] Y. Hayashi, K. Tajima, T. Kirimoto, H. Miyake, N. Matsuura, Cardioprotective effects of MET-88, a gamma-butyrobetaine hydroxylase inhibitor, on cardiac dysfunction induced by ischemia/reperfusion in isolated rat hearts, Pharmacology 61 (4) (2000) 238–243.
[14] E. Liepinsh, M. Makrecka-Kuka, E. Makarova, K. Volska, B. Svalbe, E. Sevostjanovs, S. Grinberga, J. Kuka, M. Dambrova, Decreased acylcarnitine content improves insulin sensitivity in experimental mice models of insulin resistance, Pharmacol. Res. 113 (Pt B) (2016) 788–795.
[15] R. Vilskersts, J. Kuka, E. Liepinsh, M. Makrecka-Kuka, K. Volska, E. Makarova, E. Sevostjanovs, H. Cirule, S. Grinberga, M. Dambrova, Methyl-gamma-butyrobetaine decreases levels of acylcarnitines and attenuates the development of atherosclerosis, Vasc. Pharmacol. 72 (2015) 101–107.
[16] W. Keung, J.R. Ussher, J.S. Jaswal, M. Raubenheimer, V.H. Lam, C.S. Wagg, G. D. Lopaschuk, Inhibition of carnitine palmitoyltransferase-1 activity alleviates insulin resistance in diet-induced obese mice, Diabetes 62 (3) (2013) 711–720.
[17] N. van Vlies, R. Ofman, R.J. Wanders, F.M. Vaz, Submitochondrial localization of 6-N-trimethyllysine dioxygenase - implications for carnitine biosynthesis, FEBS J. 274 (22) (2007) 5845–5851.
[18] N.R. Rose, M.A. McDonough, O.N. King, A. Kawamura, C.J. Schofield, Inhibition of 2-oxoglutarate dependent oxygenases, Chem. Soc. Rev. 40 (8) (2011) 4364–4397.
[19] M. Uhlen, L. Fagerberg, B.M. Hallstrom, C. Lindskog, P. Oksvold, A. Mardinoglu, A. Sivertsson, C. Kampf, E. Sjostedt, A. Asplund, I. Olsson, K. Edlund, E. Lundberg, S. Navani, C.A. Szigyarto, J. Odeberg, D. Djureinovic, J.O. Takanen, S. Hober, T. Alm, P.H. Edqvist, H. Berling, H. Tegel, J. Mulder, J. Rockberg, P. Nilsson, J. M. Schwenk, M. Hamsten, K. von Feilitzen, M. Forsberg, L. Persson, F. Johansson, M. Zwahlen, G. von Heijne, J. Nielsen, F. Ponten, Proteomics. Tissue-based map of the human proteome, Science 347 (6220) (2015) 1260419.
[20] J. Monfregola, G. Napolitano, I. Conte, A. Cevenini, C. Migliaccio, M. D'Urso, M. V. Ursini, Functional characterization of the TMLH gene: promoter analysis, in situ hybridization, identification and mapping of alternative splicing variants, Gene 395 (1–2) (2007) 86–97.
[21] J.C. McGrath, G.B. Drummond, E.M. McLachlan, C. Kilkenny, C.L. Wainwright, Guidelines for reporting experiments involving animals: the ARRIVE guidelines, Br. J. Pharmacol. 160 (7) (2010) 1573–1576.
[22] S.L. Menezes-Filho, I. Amigo, L.A. Luevano-Martinez, A.J. Kowaltowski, Fasting promotes functional changes in liver mitochondria, Biochim. Biophys. Acta Bioenerg. 1860 (2) (2019) 129–135.
[23] A. Kazaks, M. Makrecka-Kuka, J. Kuka, T. Voronkova, I. Akopjana, S. Grinberga, O. Pugovics, K. Tars, Expression and purification of active, stabilized trimethyllysine hydroxylase, Protein Expr. Purif. 104 (2014) 1–6.
[24] M. Makrecka-Kuka, E. Sevostjanovs, K. Vilks, K. Volska, U. Antone, J. Kuka, E. Makarova, O. Pugovics, M. Dambrova, E. Liepinsh, Plasma acylcarnitine concentrations reflect the acylcarnitine profile in cardiac tissues, Sci. Rep. 7 (1) (2017) 17528.
[25] E. Liepinsh, M. Makrecka, J. Kuka, E. Makarova, R. Vilskersts, H. Cirule, E. Sevostjanovs, S. Grinberga, O. Pugovics, M. Dambrova, The heart is better protected against myocardial infarction in the fed state compared to the fasted state, Metab. Clin. Exp. 63 (1) (2014) 127–136.
[26] J. Kuka, R. Vilskersts, H. Cirule, M. Makrecka, O. Pugovics, I. Kalvinsh, M. Dambrova, E. Liepinsh, The cardioprotective effect of mildronate is diminished after co-treatment with L-carnitine, J. Cardiovasc. Pharmacol. Therapeut. 17 (2) (2012) 215–222.
[27] E. Liepinsh, J. Kuka, M. Dambrova, Troubleshooting digital macro photography for image acquisition and the analysis of biological samples, J. Pharmacol. Toxicol. Methods 67 (2) (2013) 98–106.
[28] S.C. Kolwicz Jr., R. Tian, Assessment of cardiac function and energetics in isolated mouse hearts using 31P NMR spectroscopy, JoVE 42 (2010).
[29] M. Makrecka-Kuka, S. Korzh, K. Vilks, R. Vilskersts, H. Cirule, M. Dambrova, E. Liepinsh, Mitochondrial function in the kidney and heart, but not the brain, is mainly altered in an experimental model of endotoxaemia, Shock 52 (6) (2019) e153–e162.
[30] A.V. Berezhnov, E.I. Fedotova, M.N. Nenov, V.A. Kasymov, O.Y. Pimenov, V. V. Dynnik, Dissecting cellular mechanisms of long-chain acylcarnitines-driven cardiotoxicity: disturbance of calcium homeostasis, activation of Ca(2+)-dependent phospholipases, and mitochondrial energetics collapse, Int. J. Mol. Sci. 21 (20) (2020).
[31] Y.M. Lenighan, B.A. McNulty, H.M. Roche, Dietary fat composition: replacement of saturated fatty acids with PUFA as a public health strategy, with an emphasis on -linolenic acid, Proc. Nutr. Soc. 78 (2) (2019) 234–245.
[32] P. Korge, H.M. Honda, J.N. Weiss, Effects of fatty acids in isolated mitochondria: implications for ischemic injury and cardioprotection, Am J Physiol-Heart C 285 (1) (2003) H259–H269.
[33] L.L. Bieber, Carnitine, Annu. Rev. Biochem. 57 (1988) 261–283.
[34] J.I. Nezu, I. Tamai, A. Oku, R. Ohashi, H. Yabuuchi, N. Hashimoto, H. Nikaido, A. Sai, K. Koizumi, Y. Shoji, G. Takada, T. Matsuishi, M. Yoshino, H. Kato, T. Ohura, G. Tsujimoto, J. Hayakawa, M. Shimane, A. Tsuji, Primary systemic carnitine deficiency is caused by mutations in a gene encoding sodium ion-dependent carnitine transporter, Nat. Genet. 21 (1) (1999) 91–94.
[35] M. Almannai, M. Alfadhel, A.W. El-Hattab, Carnitine inborn errors of metabolism, Molecules 24 (18) (2019).
[36] A.G. Engel, C. Angelini, Carnitine deficiency of human skeletal muscle with associated lipid storage myopathy: a new syndrome, Science 179 (4076) (1973) 899–902.
[37] P.B. Celestino-Soper, S. Violante, E.L. Crawford, R. Luo, A.C. Lionel, E. Delaby, G. Cai, B. Sadikovic, K. Lee, C. Lo, K. Gao, R.E. Person, T.J. Moss, J.R. German, N. Huang, M. Shinawi, D. Treadwell-Deering, P. Szatmari, W. Roberts, B. Fernandez, R.J. Schroer, R.E. Stevenson, J.D. Buxbaum, C. Betancur, S. W. Scherer, S.J. Sanders, D.H. Geschwind, J.S. Sutcliffe, M.E. Hurles, R.J. Wanders, C.A. Shaw, S.M. Leal, E.H. Cook Jr., R.P. Goin-Kochel, F.M. Vaz, A.L. Beaudet, A common X-linked inborn error of carnitine biosynthesis may be a risk factor for nondysmorphic autism, Proc. Natl. Acad. Sci. U. S. A. 109 (21) (2012) 7974–7981.
[38] J.L. Martin, A.S.H. Costa, A.V. Gruszczyk, T.E. Beach, F.M. Allen, H.A. Prag, E. C. Hinchy, K. Mahbubani, M. Hamed, L. Tronci, E. Nikitopoulou, A.M. James, T. Krieg, A.J. Robinson, M.M. Huang, S.T. Caldwell, A. Logan, L. Pala, R.C. Hartley, C. Frezza, K. Saeb-Parsy, M.P. Murphy, Succinate accumulation drives ischaemia-reperfusion injury during organ transplantation, Nat Metab 1 (2019) 966–974.

[39] E. Murphy, H. Ardehali, R.S. Balaban, F. DiLisa, G.W. Dorn, R.N. Kitsis, K. Otsu, P. Ping, R. Rizzuto, M.N. Sack, D. Wallace, R.J. Youle, C.o.C.C., American heart association Council on basic cardiovascular Sciences, G. Council on functional, B. Translational, mitochondrial function, biology, and role in disease: a scientific statement from the American heart association, Circ. Res. 118 (12) (2016) 1960–1991.

[40] A. Sandor, C.L. Hoppel, Butyrobetaine availability in liver is a regulatory factor for carnitine biosynthesis in rat. Flux through butyrobetaine hydroxylase in fasting state, Eur. J. Biochem. 185 (3) (1989) 671–675.

[41] E.A. Hosein, S.J. Booth, I. Gasoi, G. Kato, Neuromuscular blocking activity and other pharmacologic properties of various carnitine derivatives, J. Pharmacol. Exp. Therapeut. 156 (3) (1967) 565–572.

[42] M. Dambrova, S. Chlopicki, E. Liepinsh, O. Kirjanova, O. Gorshkova, V.I. Kozlovski, S. Uhlen, I. Liepina, R. Petrovska, I. Kalvinsh, The methylester of gamma-butyrobetaine, but not gamma-butyrobetaine itself, induces muscarinic receptor-dependent vasodilatation, N. Schmied. Arch. Pharmacol. 369 (5) (2004) 533–539.

[43] E. Strand, E.W. Rebnord, M.R. Flygel, V. Lysne, G.F.T. Svingen, G.S. Tell, K. H. Loland, R.K. Berge, A. Svardal, O. Nygard, E.R. Pedersen, Serum carnitine metabolites and incident type 2 diabetes mellitus in patients with suspected stable Angina pectoris, J. Clin. Endocrinol. Metab. (2018).

[44] M.G. Schooneman, R.H. Houtkooper, C.E. Hollak, R.J. Wanders, F.M. Vaz, M. R. Soeters, S.M. Houten, The impact of altered carnitine availability on acylcarnitine metabolism, energy expenditure and glucose tolerance in diet-induced obese mice, Biochim. Biophys. Acta 1862 (8) (2016) 1375–1382.